

Predicting faecal indicator organisms in coastal waters using a complex nonlinear artificial intelligence model

Man-Yue Lam¹ and Reza Ahmadian²

¹School of Engineering, Cardiff University, Cardiff CF24 3AA, UK. Email: lamM7@cardiff.ac.uk

²School of Engineering, Cardiff University, Cardiff CF24 3AA

ABSTRACT

High levels of faecal indicator organisms (FIOs) at bathing water sites can cause disease and impose threats to public health. There is a need for predicting FIO levels to inform the public and reduce exposure. Data-driven models are one of the main tools being considered as predictive models. However, identifying the main inputs of the data-driven models is a major challenge in developing FIO predictor models. This paper develops a data-driven model for FIO concentration prediction based on a limited number of critical input variables. Essential variables were identified with be a combination of Gamma test and GA (Gamma-GA-test). Artificial Neural Networks (ANNs) and linear regression models were developed using these two variable identification approaches for comparison. The models were applied to a case study, and it was found that the model using the Gamma-GA test has a high potential to predict FIO levels more accurately, although this requires further investigation with different case studies. A correlation analysis was required prior to the variable identification approaches in this study. The need of this analysis highlights the significance of understanding the waterbody and the data set in the development and application of data-driven models. Models using a Gamma-GA test were more capable of predicting extreme (high) FIO concentrations, making a Gamma-GA test more suitable for a bathing water quality early warning system. The importance of nonlinearity in such predictive models was also demonstrated by the better performance of nonlinear ANN models compared

24 to linear regression models regardless of the variable identification approaches used. This paper
25 highlights the importance of nonlinearity in bathing water quality prediction and encourages further
26 utilisation of nonlinear models for this application.

27 INTRODUCTION

28 Water-borne pathogens in waterbodies cause illnesses such as gastrointestinal infection, eye
29 infection, skin complaints, and nose and throat infections (Pruss 1998; Pandey et al. 2014). Faecal
30 indicator organisms (FIO), e.g. *E Coli* and *Enterococci*, are commonly used to indicate the level
31 of pathogens in waterbodies (Dufour 1984; Pandey et al. 2014). In Europe, the European Union
32 (EU) revised Bathing Water Directive (rBWD) (European Commission 2006) requires member
33 states to monitor at least the concentrations of two FIO species in designated bathing waters for
34 compliance. The rBWD recognises short-term occasional pollution and includes provisions for
35 discounting compliance requirements when there is a predictive and warning system to alarm
36 the public of impending poor water quality. Traditionally, FIO concentrations in bathing water
37 samples are determined by culture-based methods. These methods require a minimum of 18-24
38 hour (USEPA 2010) laboratory assay. However, FIO concentrations change continuously (Boehm
39 et al. 2002; Whitman et al. 2004; Kim et al. 2004; King et al. 2021), causing culture-based warning
40 systems to give outdated water quality alerts. More rapid FIO analysis methods such as quantitative
41 polymerize chain reaction (qPCR) can determine FIO concentrations in less than 6 hours, but these
42 methods require significant up-front investments and trained personnel (Zhang et al. 2018) and still
43 cannot be used as a predictive tool. While field sampling and analysis are important, they do not
44 provide predictions to impending bathing water quality.

45 Two- and three-dimensional hydro-environmental models are commonly applied to assess FIO
46 concentrations in waterbodies. These models numerically solve the mass and momentum equations
47 of fluids as well as the fate and transport of FIOs, including decay and interaction with sediment.
48 These models have been applied in a wide range of studies (e.g. Lee and Qu 2004; Lin et al. 2008;
49 Schippmann et al. 2013; Huang et al. 2017; Abu-Bakar et al. 2017) to provide relatively accurate
50 predictions of the spatial and temporal concentration distributions of FIOs. Nevertheless, these

51 models require detailed knowledge of flow and FIOs at the boundary of the modelling domain, which
52 are generally very expensive and time consuming to acquire. Moreover, such models are usually
53 computationally demanding and require a long run time even on modern computers. Therefore,
54 using such models in real-time as a part of early warning systems is not practical.

55 Data-driven models are promising alternatives in providing timely predictions of FIOs for
56 bathing water quality warning systems due to their lower computational requirements. Such models
57 utilize data obtained by environmental sensors to predict FIO concentrations in bathing waters. The
58 public could then be warned about occasions with high FIO concentrations. The development of
59 such data-driven models requires identifying FIO predictive variables and establishing relationships
60 between these variables and FIO concentrations. These two steps have been previously conducted
61 mainly by stepwise multi-linear regression (MLR) (e.g. [Crowther et al. 2001](#); [Nevers and Whitman
2005](#); [Gonzalez et al. 2012](#); [Wyer et al. 2013b](#); [Gonzalez and Noble 2014](#)). In a stepwise MLR,
62 variables are included or excluded in a linear regression equation in a stepwise manner. Such
63 inclusion or exclusion is decided by the influence of the input variables on estimating the target
64 variables through linear regression analysis. This linear approach does not account for possible
65 nonlinear relationships which could affect predicting extremes. A promising nonlinear approach
66 is Artificial Neural Network (ANN), in which the predictive variables and FIO concentrations are
67 linked by simplified yet nonlinear network-like models ([Masters 1993](#); [Garrett 1994](#); [Russell and
Norvig 2010](#)). ANN has been applied to predict FIO concentrations in several studies e.g. [Jin and
Englande 2006](#); [He and He 2008](#); [Zhang et al. 2012](#); [Thoe et al. 2015](#); [Zhang et al. 2018](#). ANN
68 models have shown better performance in predicting extreme FIO concentration (both high and
69 low) ([Zhang et al. 2012](#)) and give higher sensitivity to poor water quality events ([Thoe et al. 2015](#))
70 compared to stepwise MLR. However, ANN models cannot identify predictive variables from a
71 data set; manual selection of predictive variables is highly dependent on the users' judgement. This
72 could be challenging in data-rich sites which will become more common as a result of enhancements
73 in sensor and implementation of digital environments. While stepwise MLR can be conducted to
74 identify predictive variables prior to ANN, stepwise MLR is not capable of identifying nonlinear
75
76
77

78 relationships between variables and FIO concentrations.

79 A nonlinear alternative method to identify predictive variables is Gamma test. Gamma test
80 determines the significance of a set of input variables in predicting the target data, e.g. FIO con-
81 centrations, by quantifying the residue variance that cannot be explained by any smooth nonlinear
82 models (Jones 2004). Gamma test does not require an assumed nonlinear function relating input
83 variables and target data a priori. On the other hand, Gamma test does not determine the nonlinear
84 model itself. To identify predictive variables in a data set, Gamma tests can be applied to each
85 possible combination of variables and choose the best combination to be the one that gives the
86 smallest residue variance. However, for data sets containing large number of variables, searching
87 the entire input combination space requires many Gamma test computations and large computa-
88 tional power. A Genetic-Algorithm (GA) model can be utilised to circumvent the need for such
89 high computational power (Jones 2004). Although a cross validation approach (Stone 1974) may
90 be applied for nonlinear variable identification, the approach usually requires *a priori* regression
91 equations or network architectures and can be computation intensive for large data sets because of
92 the increased number of networks needed for cross-comparison.

93 This paper develops a data-driven model for FIO concentration prediction based on a limited
94 number of critical input variables. Essential variables were identified with be a combination of
95 Gamma test and GA (Gamma-GA-test). This approach was compared with the stepwise MLR,
96 which has been commonly applied in water quality prediction (Crowther et al. 2001; Nevers and
97 Whitman 2005; Wyer et al. 2013b; Thoe and Lee 2014). From the variables identified by Gamma-
98 GA test and stepwise MLR, ANN and linear regression models were developed and evaluated.
99 These techniques were applied to a data-rich test site, namely Swansea Bay, UK, where a significant
100 amount of FIO and environmental data were collected. This is the first time Gamma test has been
101 applied to identify FIO predictive variables at bathing water sites. Gamma test has been applied in
102 Kashefipour et al. 2005 and Lin et al. 2008 in bathing water quality modelling, but the test was not
103 used for variable identification. The test has also been applied in Choubin and Malekian 2017 and
104 Ghaderi et al. 2019 for variable identification, but their focuses were not bathing water quality. The

105 improvements in predicting FIO concentrations using the complex model proposed in this study at
106 the case study site are highlighted.

107 **METHODOLOGY**

108 The first step in developing data-driven models is identifying the input variables. However, there
109 may be dependencies among the available variables. To identify linearly independent variables
110 amongst all available variables, a singular value decomposition-based collinearity analysis was
111 conducted. The output variables from the analysis became the input variables for the Gamma-
112 GA tests or stepwise MLRs. ANN models were developed from predictive variables identified
113 with Gamma-GA tests (GG-ANN) and stepwise MLRs (SL-ANN) respectively. Linear regression
114 models were also developed from the identified variables (GG-Linear and SL-Linear models).
115 Fig. 1 shows a flow chart of the modelling approach in this paper and the following section gives
116 further details to the aforementioned tests and models.

117 **Collinearity analysis**

118 Linear correlation may exist among the variables within the measured data set. This is referred
119 to as collinearity (Belsley et al. 1980). Correlation analysis was conducted in this paper to remove
120 redundant variables. The correlation coefficients between variable pairs were computed. When
121 the correlation coefficient was high (e.g. > 0.6), one of the variables was removed; the variable
122 to remove was selected by mechanistic-process-based judgement. Correlation analysis was also
123 conducted to determine the lag-time required for the time-lagged variables not to have a high
124 correlation with the original un-lagged variables.

125 **Gamma test and Genetic Algorithm**

126 Gamma test determines the part of the variance of target data which cannot be accounted for by
127 any smooth nonlinear models. Nevertheless, Gamma test does not determine the model itself. The
128 Gamma test is briefly explained below but further details can be found in Stefansson et al. 1997,
129 Evans and Jones 2002, and Jones 2004. Consider a data set of input variables (the independent
130 environmental variables selected by the collinearity test in this paper) \mathbf{X} and target data (FIO

131 concentrations in this paper) \mathbf{y} :

$$132 \quad \mathbf{X} = \begin{bmatrix} x_{11} & x_{21} & \cdots & x_{N1} \\ x_{12} & x_{22} & \cdots & x_{N2} \\ \vdots & \vdots & \ddots & \vdots \\ x_{1M} & x_{2M} & \cdots & x_{NM} \end{bmatrix} \quad (1)$$

$$133 \quad \mathbf{y} = \begin{bmatrix} y_1 \\ y_2 \\ \vdots \\ y_M \end{bmatrix} \quad (2)$$

134 where x_{ji} is the j -th input variable at time i ($1 \leq i \leq M$); y_i is the target data at time i . The row
135 vectors of matrix \mathbf{X} , that is:

$$136 \quad \mathbf{x}_i = [x_{1i}, x_{2i}, \dots, x_{Ni}] \quad (3)$$

137 where superscript T denotes matrix transpose, are the environmental variable data points measured
138 at time instant i ($1 \leq i \leq M$). Assume that \mathbf{x}_i and y_i are related as:

$$139 \quad y_i = f(\mathbf{x}_i) + r \quad (4)$$

140 where f is a nonlinear and smooth function; r is a random variable (i.e. noise that is excluded from
141 the input-target relationship). We define an imaginary data point \mathbf{x}'_i near \mathbf{x}_i and:

$$142 \quad \gamma = \frac{1}{2M} \sum_{i=1}^M [y(\mathbf{x}'_i) - y(\mathbf{x}_i)]^2 \quad (5)$$

143 substitute Eq. 4 into Eq. 5 and consider the Taylor expansion $f(\mathbf{x}'_i) = f(\mathbf{x}_i) + (\mathbf{x}'_i - \mathbf{x}_i) \cdot \nabla f + O(|\mathbf{x}'_i -$
144 $\mathbf{x}_i|^2)$, where ∇ is the gradient operator. Eq. 5 becomes:

$$\gamma = \frac{1}{2M} \sum_{i=1}^M [(\mathbf{x}'_i - \mathbf{x}_i) \cdot \nabla f]^2 + \frac{1}{2M} \sum_{i=1}^M (r_2 - r_1)^2 \quad (6)$$

where r_1 and r_2 are two realizations of the random variable r corresponding to $y(\mathbf{x}_i)$ and $y(\mathbf{x}'_i)$ respectively. It is obvious from Eq. 6 that if $\mathbf{x}'_i \rightarrow \mathbf{x}_i$, $\gamma \rightarrow \frac{1}{2M} \sum_{i=1}^M (r_2 - r_1)^2 = \text{Var}(r)$ where $\text{Var}(r)$ is the variance of r in probability. Note that $\text{Var}(r)$ is obtained without knowing the expression of f .

The data point \mathbf{x}'_i that is arbitrarily close to \mathbf{x}_i does not exist in the measured data set \mathbf{X} . An approach to estimate the first term in the right-hand side in Eq. 6 is required to obtain $\text{Var}(r)$ from γ . In Gamma test, \mathbf{x}'_i is replaced by $\mathbf{x}_{N[i,k]}$, the k -th nearest data point to \mathbf{x}_i . For example, $\mathbf{x}_{N[i,k=1]}$ and $\mathbf{x}_{N[i,k=2]}$ are the nearest and the second nearest points to \mathbf{x}_i . With this replacement, Eq. 6 becomes:

$$\gamma(k) = A(k)\delta(k) + \Gamma \quad (7)$$

where

$$\delta(k) = \frac{1}{M} \sum_{i=1}^M |\mathbf{x}_{N[i,k]} - \mathbf{x}_i|^2 \quad (8)$$

$$\gamma(k) = \frac{1}{2M} \sum_{i=1}^M (y_{N[i,k]} - y_i)^2 \quad (9)$$

$$A(k) = \frac{\sum_{i=1}^M [(\mathbf{x}_{N[i,k]} - \mathbf{x}_i) \cdot \nabla f]^2}{\sum_{i=1}^M |\mathbf{x}_{N[i,k]} - \mathbf{x}_i|^2} \quad (10)$$

$$\Gamma = \frac{1}{2M} \sum_{i=1}^M (r_2 - r_1)^2 = \text{Var}(r) \quad (11)$$

where $|\cdot|$ denotes Euclidean distance; $y_{N[i,k]}$ is the target value associated with $\mathbf{x}_{N[i,k]}$ (note that $y_{N[i,k]}$ is not necessarily the k -th nearest point to y_i in the data set). [Evans and Jones 2002](#) showed that $A(k) = A$ is a constant given M is sufficiently large. Eq. 7 becomes:

$$\gamma(k) = A\delta(k) + \Gamma \quad (12)$$

A and Γ in Eq. 12 can be obtained by conducting linear regression with $\gamma(k)$ and $\delta(k)$ computed from the k -th nearest points to \mathbf{x}_i for $i = 1, \dots, M$ and $k = 1, \dots, p$ where p is the maximum value of k used. In this study, $p = 10$ as suggested by Jones 2004. $\mathbf{x}_{N[i,k]}$ for each \mathbf{x}_i in $\gamma(k)$ and $\delta(k)$ are obtained by an efficient k -dimensional tree approach (computational time in the order of $M \log M$) in Bentley 1975.

Gamma tests need to be applied to all possible combinations of input variables in order to identify the strongest predictive variables from all available data. This is the combination which gives the lowest absolute value of Γ (i.e. the combination of input variables that gives the smallest noise variance). However, this approach is computationally demanding for large data sets; the number of possible combinations for a data set of m variables is $2^m - 1$. To circumvent the need for high computational power, the variable selection problem is expressed as a minimization problem which is solved using GA (Jones 2004). The combination of input variables that minimizes $|\Gamma|$ is selected as the solution. Combinations of input variables in the GA model are represented by a binary vector of length N (a mask) in which the inclusion or exclusion of a variable is indicated by 1 or 0, respectively. In this work, the GA function "ga" in MATLAB Global Optimization Toolbox (Mathworks 2020b) is used. Readers are also referred to Deb 2000 and Deep et al. 2009 for the detail of the GA approach.

M-test (Jones 2004) can be used to determine the minimum required length of the input and target data set, the value of M in Eq. 1. This value of M is also the minimum data length required for model training if a nonlinear model is applied to the data set. In an M-test, Gamma tests are conducted sequentially with progressively increasing M . The computed $|\Gamma|$ is plotted against data length. The minimum required M is the value of M beyond which $|\Gamma|$ becomes constant. M-test results are expected to be different when the ordering of the data is different. In this work, the data order was randomly generated and three different realizations (Realization 1, 2 and 3) of data in different order was tested to reduce reliance on the order of the data.

Artificial Neural Network (ANN)

Feedforward back-propagation ANN models were used to predict Faecal Indicator Organism concentrations, including *Enterococci* and *E Coli*, based on the predictive variables selected by the Gamma-GA tests. Each network consists of an input layer, an output layer, and one hidden layer. One hidden layer suffices in this case since Masters 1993 showed that networks with one hidden layer are generally capable of approximating most underlying functions. The authors also tested GG-ANN and SL-ANN networks with two hidden layers and no significant improvement in performance was obtained compared to one-hidden-layer networks. The number of nodes required in the hidden layer was determined by experimentation to give the best results without overfitting.

The networks were trained and validated with the ANN function "train" in MATLAB deep learning toolbox (Mathworks 2020a). To retain a portion of the data for model validation and to avoid over-training, the data set was divided to three sets, namely the training, validation, and testing sets. For each of the three realizations in the M-test, the data were grouped into the three sets according to the data order (i.e. the 1st to n th data were put into the training set; the $n + 1$ -th to m -th data were put into the validation set; the $m + 1$ -th to the end of the data were put into the testing set; $n < m$). The performance function used in this study was the mean squared error (MSE) between model outputs and target data. Training of a network was stopped when no further improvement in MSE for the validation data set can be achieved after six iterations. While this method avoids parameter (weights and bias) over-training, it does not avoid over-training due to over-complicated network architecture and redundant predictive variables. For each network, 300 training runs with random initial weights were conducted and the network that provided the minimum MSE was chosen. (Iyer and Rhinehart 1999) showed that the network obtained from this approach has a 95% confidence level that its MSE is within the lowest 1.0%.

Linear regression models with their predictive variables selected by the Gamma-GA tests (GG-Linear models) and stepwise MLR models (SL-Linear models) were also developed to assess ANN model performance.

MODEL APPLICATION

The model was applied to Swansea Bay, located on the north of the Bristol Channel in the South West of the UK, as shown in Fig. 2a. Along the bay are two sandy beaches with bathing water status: the Swansea Beach and the Aberavon Beach. Potential sources of FIO in the Bay are the discharges from rivers, streams, surface water drains, three offshore outfalls from wastewater treatment works, and transport by currents from sources outside of the Bay. Large amount of data were collected as a part of the previous Smart Coast Sustainable Communities (SCSC) research project (Wyer et al. 2013b, Wyer et al. 2018) which alongside the variety of the sources make the bay an ideal case study for data-driven modelling. The stream and drain discharges are generally low ($< 1m^3/s$); River Tawe, Clyne, Neath, and Afan have relatively high flow rates ($> 5m^3/s$). The water is well mixed in the Severn Estuary and Bristol Channel (Uncles 1981; Evans et al. 1990; Ahmadian et al. 2013). FIO concentrations in the beaches are governed by the sources and the hydrodynamics in the Bay (Ahmadian et al. 2013).

The concentrations of two FIO species, namely *E Coli* and *Enterococci*, were sampled at various sources and receptors at high frequency, i.e. intervals of 15-30 min, in year 2011 and 2012. In Swansea Beach, the large tidal range (exceeding 10 m) and sloping beach results in a tidal flat exposed up to 1500 m from shore during high spring tides. The large extent of the tidal flats makes single point FIO concentration measurement impossible. In the data collection scheme, FIO concentrations were measured along a sampling transect consisting of Designated Sampling Points (DSPs) in Swansea Bay, as shown in Fig. 2a. Fig. 2b shows the DSPs in the sampling transect in the 2011 bathing season. Environmental variables such as stream flow, tidal, meteorological, and water quality data at the locations are also shown in Fig. 2a. The samples were collected in sterile 1 L containers (Aurora Scientific) and stored in a refrigerator before analysis. The samples were then analysed for intestinal *Enterococci* and *E Coli* with standard membrane filtration techniques and analysed for turbidity with a bench turbidity meter (Hannah Instruments LP2000). Salinity was also measured with a conductivity meter (Mettler Toledo SevenGo). Fig. 2a also shows the sampling locations of the environmental variables in the SCSC project. Tide level and the flow rates at river

246 Tawe, Neath and Afan were measured by the existing gauges in the hydrometric monitoring network
 247 operated by Natural Resources Wales (NRW), the official natural resource management organisation
 248 in Wales. The water depths and velocities at the five smaller streams were measured by pressure
 249 transducers (OTT Orpheus Mini) and electro-magnetic velocity meters (Sensa RC2) respectively.
 250 Global radiation, temperature, relative humidity, rainfall, and wind speed were measured at the
 251 meteorological station. Global radiation was measured by a pyranometer (Skye Instruments SKS
 252 1110); air temperature and relative humidity were measured by a sensor (Rotronic HygroClip2
 253 HC2-S3); rainfall was measured with a tipping bucket rain gauge (Met One Instruments 370C 20.3
 254 cm aperture, 0.2 mm tip); Wind speed and direction were measured with an anemometer (Gill
 255 Instruments WindSonic). Offshore wastewater discharge volumes were also measured in the SCSC
 256 project but were not included as potential model outputs because the tracer study conducted as a part
 257 of the SCSC project (Ahmadian et al. 2013) and the two-dimensional TELEMAC hydrodynamic
 258 simulation conducted by the authors suggested that they are not important for FIO concentrations
 259 at the DSPs compared to other FIO sources (not shown).

260 Table 1 and 2 summarises the data set used in this paper. The target variables were *Enterococci*
 261 and *E Coli* concentrations measured at the Bathing Water Designated Sampling Points (DSPs)
 262 during a bathing season, namely 22 June to 28 September, 2011. The input data set included 16
 263 environmental variables measured in the same bathing season as shown in Table 2. The range
 264 of values of different input and target variables were significantly different, as shown in Table 1
 265 and 2, due to the large number of factors that affects bacteria concentrations. In order to ensure
 266 consistency between data and reduce the impact of variation ranges on the model, all the data have
 267 been normalized to the range of 0-1 using the following equation:

$$268 \quad x_{j,nor} = \frac{x_j - x_{j,min}}{x_{j,max} - x_{j,min}} \quad (13)$$

269 where x_j and $x_{j,nor}$ are the un-normalized and normalized j -th variable; $x_{j,max}$ and $x_{j,min}$ are
 270 the maximum and minimum of the time series x_j , before data processing and model training.
 271 Logarithmic transformation was applied to the variables that have relatively high skewness to

272 transform them from a lognormal-like distribution to a normal-like distribution. This transformation
273 is necessary because stepwise-MLR models assume normally distributed data (skewness=0). If the
274 data has a significant skewness, the stepwise-MLR variable inclusion/exclusion procedures may not
275 be suitable and subsequently the model would not result in good validation. Collinearities among
276 variables were identified and redundant variables were removed. In order to build memory of the
277 past conditions, e.g. solar radiation or rain prior to the simulation, and time required for transport
278 of bacteria across the bay, which could significantly affect the concentration of bacteria, in the
279 data-driven model, time-lagged variables were also considered as the input variables. Correlation
280 analysis was conducted to identify collinear variables and determine and lag time that does not
281 cause additional collinearity issues.

282 **RESULTS AND DISCUSSION**

283 **Input variable selection**

284 From the correlation analysis, 23 input variables were identified as shown in the column
285 “Variables identified from the correlation analysis” in Table 3. Only one single representative
286 stream flow, the flow of the Tawe River, was selected since flows at different streams with no time
287 lag were found highly correlated. Such a high correlation could be explained by the small size
288 of catchment associated with each stream, which means all streams are influenced with similar
289 weather, and particularly rainfall, patterns. [Burton et al. 2013](#) reported that the spatial correlation
290 of rainfall at the site remains higher than 0.5 for two points that are 100 km apart, implying that the
291 rainfall is correlated within a $100 \times 100 = 10,000 \text{ km}^2$ area. This area is larger than the sum of the
292 watersheds of three major rivers discharging to the Bay (506.4 km^2), namely the watershed for River
293 Tawe (227.7 km^2), River Neath (190.9 km^2), and River Afan (87.8 km^2). Turbidity and salinity
294 were also found highly correlated with the streamflow and thus eliminated from the data set. This
295 is consistent with the idea in [Thoe and Lee 2014](#) that salinity reflects the mixing between riverine
296 freshwater and the ambient sea water. The correlation analysis also shows high correlations between
297 a time-lagged variable and the same variable with no time-lag if the time lag is not sufficiently long
298 as expected. The correlation between the no time-lag and time-lagged streamflow remains high (>

299 0.6) for a lag time from 0.25-36 hours; only the streamflow with 10-hour lag was selected following
300 hydrodynamic model results (Lam and Ahmadian 2022). For other variables, the minimum time-
301 lag from the FIO data was 2 hours to render the AI model predictive. Additional time-lags were
302 applied to these variables at suitable time intervals such that the correlations between time-lagged
303 and unlagged variables were not significant (< 0.6). The time intervals determined by correlation
304 analysis were as follows: 2 hours for tides; 2 hours for radiation; 6 hours for humidity; 0.25-hour
305 intervals for rainfall; 4 hours for temperature; 4 hours for wind speed N; 8 hours for wind speed
306 E. Table 3 shows that the time interval for rainfall is greater than 0.25-hour; it is because rainfall
307 was not expected to have an immediate effect on FIO concentrations from physical process point
308 of view.

309 Table 3 shows the predictive variables identified by the Gamma-GA tests and stepwise MLRs.
310 For consistency of comparison between the methods and prevent over-paramatization, both Gamma-
311 GA tests and stepwise MLRs were constrained to choose a maximum of eight variables. Ideally,
312 an interpretability analysis of the variables identified by Gamma-GA tests and stepwise MLRs is
313 desirable to assess the performance of Gamma-GA tests, but such comparison requires a priori
314 knowledge about the relative importance of the variables in the site, which is not available to date.
315 Nevertheless, the physical plausibility of the selected variables is discussed as follows. Tide level
316 was selected to be an important variable by both Gamma-GA tests and stepwise-MLR models. The
317 results are consistent with the fact that tides were shown important to the flow in Swansea Bay
318 (Ahmadian et al. 2013) as well as FIO concentrations (Lam and Ahmadian 2022). Tides were also
319 identified as an important variable in other data-driven models for other nearshore coastal waters
320 (Crowther et al. 2001; Nevers and Whitman 2005; He and He 2008; Zhang et al. 2012). Wind was
321 also shown important for FIO concentration by both predictive variable identification methods. It
322 is consistent with the stepwise-MLR results in Wyer et al. 2013b. Streamflow, as a known FIO
323 source (e.g. Wyer et al. 2010; Wyer et al. 2013a; Lam and Ahmadian 2022), was included by
324 only Gamma-GA model for *Enterococci* but the variable was not included for other tests. This is
325 attributed to the small spatial and temporal scale (in a watershed of about 500 km² and sampling

326 interval of 30 minutes) of the site. In this study, flow rates of different rivers under a time lag
327 of less than 36 hours are highly correlated and one representative streamflow (River Tawe) at one
328 particular time lag (10 hours) was selected. Information concerning the exact riverine FIO sources
329 for the measured FIO concentration was lost. In summary, Gamma-GA test can identify predictive
330 variables that are consistent with the literature.

331 **M-test**

332 M-test was conducted for variables identified by the Gamma-GA tests and stepwise MLRs to
333 determine the data length needed for model training. Fig. 3 shows that the Gamma-GA tests selected
334 variables that achieve lower (i.e. better) $|\Gamma|$ compared to the stepwise MLRs given a sufficiently
335 long data (e.g. beyond 500 data points) which means that the data length for model training
336 should be greater than 200 for Gamma-GA test to give better results compared with stepwise MLR.
337 Following the M-test, the ratio of data points in training, validation and testing sets is 0.6:0.2:0.2,
338 giving $949 \times 0.6 = 571$ data points in the training set, which satisfies the minimum of 200 data
339 points imposed by the M-test. The mean and standard deviation values of the training, validation,
340 and testing data sets are checked to be approximately comparable in all three realizations.

341 **ANN model results**

342 *Selection of number of nodes*

343 Fig. 4 shows a typical relationship between MSE and number of hidden layer node for *Entero-*
344 *cocci*. SL-ANN models reached lower MSEs when there were few nodes in the hidden layer. As
345 there were more hidden layer nodes (>10), GG-ANN models achieved better performance. For *E*
346 *Coli*, Fig. 5 shows that GG-ANN and SL-ANN models gave similar MSEs. The fact that GG-ANN
347 and SL-ANN models gave similar MSEs does not conflict with the M-test results. Although the
348 M-test results suggested that the Gamma-GA tests identified variables had the potential to achieve
349 lower MSEs, M-test does not specify the nonlinear model that gives such results. It is possible
350 that other nonlinear models other than ANN give better results in comparison to the Gamma-GA,
351 however, this is out of the scope of this study. For further comparison between models developed
352 from the Gamma-GA tests and stepwise MLRs, networks with 1 to 50 nodes in the hidden layer

353 were tested and the number of nodes in the hidden layer was selected based on providing the lowest
354 validation MSE. The MSE resulting from different networks with a different number of nodes in
355 the hidden layer is illustrated in Fig. 4 and 5.

356 *Mean squared error (MSE) and R^2*

357 Fig. 6 and 7 show the comparison between GG-ANN model results and target FIO concentrations
358 for training, validation, and test data sets, as well as all data. Table 4 and 5 show the comparison
359 between GG-ANN, SL-ANN, GG-Linear, and SL-Linear models. For most ANN models, the
360 optimal SL-ANN models consisted of fewer hidden layer nodes compared to GG-ANN models,
361 which is consistent with the section "Selection of number of nodes". GG-ANN and SL-ANN
362 models gave better MSE and R^2 than GG-Linear and SL-Linear models. This shows the capacity
363 of nonlinear models in capturing inherent nonlinear relationships between variables and FIO
364 concentrations. GG-ANN models gave better training, validation, and testing results than SL-ANN
365 models for *Enterococci*, but SL-ANN models gave better validation and testing results for *E Coli*.
366 The better GG-ANN performance for *Enterococci* can be explained by the fact that GG-ANN better
367 captures extreme FIO concentrations as illustrated in section "Performance Table". This GG-ANN
368 property helps the models perform better for *Enterococci* because there are more extreme values
369 for the data series of *Enterococci* (17.8% of the data was below 0.1 or above 0.9) compared to *E*
370 *Coli* (8.9% of the data was below 0.1 or above 0.9). The MSE of SL-Linear models was better
371 than the one of the GG-Linear models, verifying the fact that stepwise MLR chooses variables that
372 optimize linear model performance compared to Gamma-GA test.

373 *Performance tables*

374 The ability to identify the most hazardous circumstances, namely poor water quality conditions,
375 are particularly important when a real-time predictive model is used as an early warning system.
376 The EU rBWD (European Commission 2006) considers the water quality in a bathing site "poor" if
377 the 90-percentile FIO concentration in the log-normal distribution obtained from the last assessment
378 period (usually the last four bathing seasons) exceeds a given threshold. The threshold is 185 cfu/100
379 mL for *Enterococci* and 500 cfu/100 mL for *E Coli*. In this study, the use of 90-percentile values is

380 not sensible since water quality is being predicted at a 30-minute interval. To test the models' ability
381 to identify poor water quality events, individual *Enterococci* and *E Coli* concentration values were
382 compared to the 185 cfu/100 mL and 500 cfu/100 mL thresholds, respectively. Fig. 8 shows the
383 performance tables of the data-driven models in correctly predicting poor water quality under the
384 EU rBWD classification for the testing sets. In this context, sensitivity and specificity are defined
385 as:

$$386 \quad \text{Sensitivity} = \frac{\text{Correctly predicted poor water quality}}{\text{Observed poor water quality}} \quad (14)$$

$$387 \quad \text{Specificity} = \frac{\text{Correctly predicted not poor water quality}}{\text{Observed not poor water quality}} \quad (15)$$

389 To explain, sensitivity represents the likelihood that a poor water quality event is correctly predicted.
390 Specificity represents the likelihood that a "not poor" water quality event is correctly predicted.
391 It can be alternatively interpreted as a minus false alarm rate. Being consistent with the result
392 that the ANN models gave better MSE and R^2 values, the ANN models gave significantly higher
393 sensitivity than the linear regression models: 24-62% and 0%-14% respectively. The observation
394 that nonlinear models give more accurate FIO predictions is consistent with [Thoe et al. 2015](#). The
395 results are also consistent with [Zhang et al. 2012](#) that ANNs capture extreme FIO values better than
396 linear regression models. Sensitivities of GG-ANN models were higher than the ones for SL-ANN
397 models for both *Enterococci* and *E Coli*, despite the MSEs for SL-ANN models being lower than
398 the ones for GG-ANN models for *E Coli*. It suggests that GG-ANN models better capture high
399 FIO concentrations compared to SL-ANN models. The sensitivity of SL-Linear models was better
400 than the one of GG-Linear models as expected from the MSE and R^2 results. Specificities for all
401 the models tested were always higher than 90%. This is probably due to the small proportion of
402 poor water quality events during the study period.

403 Sensitivity was higher for *Enterococci* concentrations than for *E Coli* in Fig. 8 for GGANN
404 models. The same was observed in the performance tables for the entire data set (949 data points).
405 An explanation can be given from the probability distribution of the *Enterococci* and *E Coli* data.

406 A Chi-square test showed that both data follow lognormal distributions with a confidence level of
407 above 95% if very small values (<3 cfu/100 mL) were removed. From the respective probability
408 distribution functions, the exceedance probability of the *Enterococci* threshold (15.9%) was higher
409 than the one of *E Coli* (5.5%) from the entire data set. With a lower exceedance probability, models
410 that better capture extreme values are required to achieve a better sensitivity for *E Coli* compared
411 to *Enterococci* concentrations.

412 DISCUSSION

413 Gamma test is a promising tool to identify input data for a data-driven model because it is
414 nonlinear, and it does not require a regression equation a priori. Nevertheless, these advantages
415 do not imply that Gamma tests can be applied with no knowledge about the waterbody or the
416 data to which the test is applied. In this paper, a correlation analysis was conducted prior to the
417 Gamma-GA tests to remove highly correlated candidate predictive variables.

418 The GG-ANN and SL-ANN models fitted better to the measured FIO concentrations and
419 captured better the extreme FIO concentrations compared to GG-Linear and SL-Linear models.
420 This is consistent with Zhang et al. 2012 for FIO concentrations and Keiner and Yan 1998 for
421 chlorophyll-a and suspended sediments. While Zhang et al. 2012 arrived at this conclusion by
422 comparing 15-variable ANN models to 5 or 6-variable linear regression models, this study confirms
423 their findings with the same number of explanatory variables used in the ANN and linear models.
424 This demonstrates the importance of including nonlinearity in capturing high FIO concentrations.
425 The effect of nonlinearity of ANN is also reflected in higher sensitivities of GG-ANN and SL-
426 ANN models compared to GG-Linear and SL-Linear models. Comparing GG-ANN and SL-ANN
427 models, GG-ANN models gave better results for *Enterococci* for all training, validation and testing
428 sets and most of the training sets for *E Coli*. While SL-ANN models gave better testing results
429 for *E Coli*, GG-ANN models gave higher sensitivities for both *Enterococci* and *E Coli*, showing
430 that Gamma-GA models select variables that capture better extreme FIO concentrations compared
431 to the stepwise MLR. The results suggest that GG-ANN model is more suitable for bathing water
432 quality warning applications in which predicting high FIO concentrations is the major concern.

433 This paper presented a GG-ANN model training and validation framework which is generally
434 applicable to different sites, although a new GG-ANN model development is required for every new
435 study. Once the GG-ANN model is developed, it can discern critical parameters from redundant
436 parameters for water quality prediction and to keep the sampling cost of running the model in
437 real-time limited by only measuring critical parameters. The data used in this paper had a very
438 short (0.5 hr) sampling interval, while the commonly used sampling intervals are usually in the
439 order of days (He and He 2008; Zhang et al. 2012; Thoe et al. 2015; Zhang et al. 2018). The
440 models used in this paper generally gave lower R^2 than the daily predictions of water quality in the
441 literature. This highlights the difficulty of short-term water quality prediction; further study of the
442 effect of time-scale on prediction accuracy is needed. While Zhang et al. 2018 attempted to predict
443 water quality with ANN at different time-scales, their results were not conclusive. Nevertheless,
444 this paper highlights the potential for a combination of Gamma-GA test and a nonlinear predictive
445 model to give timely bathing water quality prediction. This can be used as early warning systems
446 on impending poor water quality together with real-time environmental sensors.

447 CONCLUSION

448 This paper develops a data-driven model for FIO concentration prediction with only limited
449 number of critical and without unnecessary input variables. The performance of Gamma-GA test
450 as a tool for predictive variable identification of *Enterococci* and *E Coli* at interval of 30 minutes
451 was evaluated. ANN and linear regression models were developed from the variables identified
452 from Gamma-GA test and stepwise MLR for comparison. The GG-ANN models gave better results
453 for *Enterococci* for all training, validation and testing sets and most of the training sets for *E Coli*.
454 The results also demonstrated the potential for Gamma-GA test to identify variables that give a
455 better model compared to stepwise MLR. While SL-ANN models usually gave better MSE and R^2
456 for testing results of *E Coli*, GG-ANN model was better in identifying events of poor water quality.
457 This illustrates the merit of nonlinear variable identification approach – the variables identified are
458 more capable of predicting high FIO concentrations. Therefore, GG-ANN model is more suitable
459 for bathing water warning applications in which predicting high FIO concentrations is the major

460 concern. For the two variable identification approaches, ANN models were better than linear
461 regression models in terms of MSE, R^2 as well as sensitivity. This result again highlighted the
462 importance of including nonlinear effects in prediction models.

463 In conclusion, this paper demonstrated the potential of combining Gamma-GA test and ANN
464 to predict bathing water quality. Prior to the variable identification tests, a correlation analysis was
465 conducted to remove redundant variables in the data set. The need of such an analysis illustrates
466 the importance of understanding the data set in the development and application of data-driven
467 models.

468 **DATA AVAILABILITY STATEMENT**

469 Some data, models, or codes that support the findings of this study are available from the
470 corresponding author upon reasonable request (The MATLAB codes for Gamma-GA tests and
471 the ANN models and the model outputs). The bacteria and environmental data were collected by
472 Aberystwyth University, Swansea City Council and Natural Resources Wales (Environmental Pro-
473 tection and Regulatory Authority in Wales) and unfortunately the authors have not been authorized
474 to share the data set.

475 **ACKNOWLEDGEMENTS**

476 The study is carried out as a part of the EERES4WATER (Promoting Energy-Water nexus
477 resource efficiency through renewable energy and energy efficiency) project, which is co-financed
478 by the Interreg Atlantic Area Programme through the European Regional Development Fund under
479 EAPA 1058/2018.

480 **NOTATION**

481

The following symbols are used in this paper:

A = the slope for the Gamma test regression equation;

$f(\cdot)$ = the nonlinear smooth function relating \mathbf{x}_i and y_i ;

M = the total number of time instants of the data;

r = random variable (noise);

\mathbf{X} = the linearly independent environmental variables;

\mathbf{x}_i = the linearly independent environmental variables at time instant i (i.e. the data point at i);

\mathbf{x}'_i = the imaginary environmental variables at time instant i ;

$\mathbf{x}_{N[i,k]}$ = the k -th nearest data point to \mathbf{x}_i ;

482

x_j = the j -th environmental variable;

$x_{j,nor}$ = the normalized x_j ;

$x_{j,max}$ = the maximum value of variable x_j ;

$x_{j,min}$ = the minimum value of variable x_j ;

\mathbf{y} = target data (FIO concentrations);

$y_{N[i,k]}$ = the target data value associated with $\mathbf{x}_{N[i,k]}$;

γ = an estimate of variability among \mathbf{x}_i , $1 \leq i \leq M$;

Γ = the intercept for the Gamma test regression;

δ = an estimate of variability among y_i , $1 \leq i \leq M$

483

REFERENCES

484

Abu-Bakar, A., Ahmadian, R., and Falconer, R. A. (2017). "Modelling the transport and decay processes of microbial tracers in a macro-tidal estuary." *Water Res.*, 123, 802–824.

485

486

Ahmadian, R., Bomminayuni, S., Falconer, R., and Stoesser, T. (2013). "Numerical modelling of flow and faecal indicator organism transport at swansea bay, uk." *A report from the interreg 4a smart coasts – sustainable communities project.*

487

488

489

Belsley, D. A., Kuh, E., and Welsch, R. E. (1980). *Regression diagnostics: Identifying influential data and sources of collinearity.* John Wiley and Sons, USA.

490

491 Bentley, J. (1975). "Multidimensional binary search trees used for associative search." *Comm ACM*,
492 18, 309–517.

493 Boehm, A. B., Grant, S. B., Kim, J. H., Mowbray, S. L., McGee, C. D., Clark, C. D., Foley, D. M.,
494 and Wellman, D. E. (2002). "Decadal and shorter period variability of surf zone water quality at
495 huntington beach, california." *Environ. Sci. Technol.*, 36(18), 3885–3892.

496 Burton, A., Glenis, V., Jones, M. R., and Kilsby, C. G. (2013). "Models of daily rainfall cross-
497 correlation for the united kingdom." *Environmental Modelling and Software*, 49, 22–33.

498 Choubin, B. and Malekian, A. (2017). "Combined gamma and m-test-based ann and arima models
499 for groundwater fluctuation forecasting in semiarid regions." *Environ. Earth Sci.*, 76, 538.

500 Crowther, J., Kay, D., and Wyer, M. D. (2001). "Relationships between microbial water quality
501 and environmental conditions in coastal recreational waters: The fylde coast, uk." *Water Res.*,
502 35(17), 4029–4038.

503 Deb, K. (2000). "An efficient constraint handling method for genetic algorithms." *Comput. Methods*
504 *Appl. Mech. Engrg.*, 186, 311–338.

505 Deep, K., Singh, K. P., Kansal, M. L., and Mohan, C. (2009). "A real coded genetic algorithm for
506 solving integer and mixed integer optimization problems." *Applied Mathematics and Computa-*
507 *tion*, 212(2), 505–518.

508 Dufour, A. P. (1984). "Bacterial indicators of recreational water quality." *Canadian journal of*
509 *public health*, 75(1), 49–56.

510 European Commission (2006). "Directive 2006/7/EC of the european parliament and of the council
511 of 15 february 2006 concerning the management of bathing water quality and repealing directive
512 76/160/EEC." *OJEU*, 64, 37–51.

513 Evans, D. and Jones, A. J. (2002). "A proof of the gamma test." *Proc R Soc Lond A*, 458, 2759–2799.

514 Evans, G. P., Mollowney, B. M., and Spoel, N. C. (1990). "Two-dimensional modelling of the
515 bristol channel, uk." *Proceedings of the conference on estuarine and coastal modelling*, S. ML,
516 ed., 331–340.

517 Garrett, J. J. (1994). "Where and why artificial neural networks are applicable in civil engineering."

518 *J Comput. Civil Eng., ASCE*, 8(2), 129–130.

519 Ghaderi, K., Motamedvaziri, B., Vafakhah, M., and Dehghani, A. A. (2019). “Regional flood
520 frequency modeling: a comparative study among several data-driven models.” *Arab J Geosci*,
521 12, 588.

522 Gonzalez, R. A., Conn, K. E., Crosswell, J. R., and Noble, R. T. (2012). “Application of empirical
523 predictive modeling using conventional and alternative fecal indicator bacteria in eastern north
524 carolina waters.” *Water Res.*, 46, 5871–5882.

525 Gonzalez, R. A. and Noble, R. T. (2014). “Comparisons of statistical models to predict fecal
526 indicator bacteria concentrations enumerated by qpcr- and culture-based methods.” *Water Res.*,
527 48, 296–305.

528 He, L. M. and He, Z. L. (2008). “Water quality prediction of marine recreational beaches receiving
529 watershed baseflow and stormwater runoff in southern california, usa.” *Water Res.*, 42, 2563–
530 2573.

531 Huang, G., Falconer, R. A., and Lin, B. (2017). “Integrated hydro-bacterial modelling for predicting
532 bathing water quality.” *Estuarine, Coastal and Shelf Science*, 188, 145–155.

533 Iyer, M. S. and Rhinehart, R. R. (1999). “A method to determine the required number of neural-
534 network training repetitions.” *IEEE T. Neural Networ.*, 10(2), 427–432.

535 Jin, G. and Englande, A. J. (2006). “Prediction of swimmability in a brackish water body.” *Man-
536 agement of Environmental Quality*, 17(2), 197–208.

537 Jones, A. J. (2004). “New tools in non-linear modelling and prediction.” *CMS*, 1, 109–149.

538 Kashefipour, S. M., Lin, B., and Falconer, R. A. (2005). “Neural networks for predicting seawater
539 bacterial levels.” *P. I. Civil Eng-Wat M.*, 158(3), 111–118.

540 Keiner, L. E. and Yan, X. (1998). “A neural network model for estimating sea surface chlorophyll
541 and sediments from thematic mapper imagery.” *Remote Sens. Environ.*, 66, 153–165.

542 Kim, J. H., Grant, S. B., McGee, C. D., Sanders, B. F., and Largier, J. L. (2004). “Locating sources
543 of surf zone pollution: A mass budget analysis of fecal indicator bacteria at huntington beach,
544 california.” *Environ. Sci. Technol.*, 38(9), 2626–2636.

545 King, J., Ahmadian, R., and Falconer, R. (2021). “Hydro-epidemiological modelling of bacterial
546 transport and decay in nearshore coastal waters.” *Water Res.*, 196, 117049.

547 Lam, M. Y. and Ahmadian, R. (2022). “Numerical source-receptor connectivity study in nearshore
548 coastal waters.” *Proceedings of the 39th IAHR World Congress, Guadiana, Spain, 19-24 Jun.*

549 Lee, J. and Qu, B. (2004). “Hydrodynamic tracking of the massive spring 1998 red tide in hong
550 kong.” *J. Environ. Eng., ASCE*, 130(5), 535–550.

551 Lin, B., Syed, M., and Falconer, R. A. (2008). “Predicting faecal indicator levels in estuarine
552 receiving waters - an integrated hydrodynamic and ann modelling approach.” *Environ. Modell.*
553 *Softw.*, 23, 729–740.

554 Masters, T. (1993). *Practical Neural Network Recipes in C++*. Academic, San Diego, CA.

555 Mathworks (2020a). *MATLAB Deep learning toolbox user’s guide*. Massachusetts, USA.

556 Mathworks (2020b). *MATLAB Global optimization toolbox user’s guide*. Massachusetts, USA.

557 Nevers, M. B. and Whitman, R. L. (2005). “Nowcast modeling of escherichia coli concentrations
558 at multiple urban beaches of southern lake michigan.” *Water Res.*, 39, 5250–5260.

559 Pandey, P. K., Kass, P. H., Soupir, M. L., Biswas, S., and Singh, V. (2014). “Contamination of
560 water resources by pathogenic bacteria.” *AMB Express*, 4(51), 5250–5260.

561 Pruss, A. (1998). “Review of epidemiological studies on health effects from exposure to recreational
562 water.” *International Journal of Epidemiology*, 27, 1–9.

563 Russell, S. J. and Norvig, P. (2010). *Artificial intelligence - a modern approach*. Pearson, England,
564 3rd edition edition.

565 Schippmann, B., Schernewhki, G., and Grawe, U. (2013). “Escherichia coli pollution in a baltic sea
566 lagoon: A model-based source and spatial risk assessment.” *International Journal of Hygiene*
567 *and Environmental Health*, 216, 408–420.

568 Stefansson, A., Koncar, N., and Jones, A. J. (1997). “A note on the gamma test.” *Neural Comput*
569 *and Applic*, 5, 131–133.

570 Stone, M. (1974). “Cross-validatory choice and assessment of statistical predictions.” *J R Stat Soc*
571 *Series B*, 36, 117–147.

572 Thoe, W., Gold, M., Griesbach, A., Grimmer, M., Taggart, M. L., and Boehm, A. B. (2015). “Sunny
573 with a chance of gastroenteritis: Predicting swimmer risk at california beaches.” *Environ. Sci.*
574 *Technol.*, 49, 423–431.

575 Thoe, W. and Lee, J. H. W. (2014). “Daily forecasting of hong kong beach water quality by multiple
576 linear regression models.” *J Environ Eng, ASCE*, 140(2), 04013007.

577 Uncles, R. J. (1981). “A numerical simulation of the vertical and horizontal m2 tide in the bristol
578 channel and comparisons with observed data.” *Limnology and Oceanography*, 26, 571–577.

579 USEPA (2010). “Predictive tools for beach notification, vol i: Review and technical protocol.”
580 *Report No. EPA-823-R-10-003*, USEPA.

581 Whitman, R. L., Nevers, M. B., Korinek, G. C., and Byappanahalli, M. N. (2004). “Solar and
582 temporal effects on escherichia coli concentration at a lake michigan swimming beach.” *Appl.*
583 *Environ. Microbial.*, 70(7), 4276–4285.

584 Wyer, M. D., Kay, D., Morgan, H., Naylor, S., Clark, S., Govier, P., Watkins, J., Davies, C., Francis,
585 C., Jones, J., Palmer, C., and Kay, C. (2013a). “Faecal indicator source connectivity for inputs to
586 swansea bay, south wales, uk, a report from the interreg 4a smart coasts-sustainable communities
587 project.” *Report no.*

588 Wyer, M. D., Kay, D., Morgan, H., Naylor, S., Clark, S., Watkins, J., Davies, C. M., Francis,
589 C., Osborn, H., and Bennett, S. (2018). “Within-day variability in microbial concentrations at
590 a uk designated bathing water: Implications for regulatory monitoring and the application of
591 predictive modelling based on historical compliance data.” *Water Res. X*, 1, 100006.

592 Wyer, M. D., Kay, D., Morgan, H., Naylor, S., Govier, P., Clark, S., Watkins, J., Davies, C. M.,
593 Francis, C., Osborn, H., and Bennett, S. (2013b). “Statistical modelling of faecal indicator
594 organisms at a marine bathing water site: results of an intensive study at swansea bay, uk: A
595 report from the interreg 4a smart coasts – sustainable communities project.” *Report no.*

596 Wyer, M. D., Kay, D., Watkins, J., Davies, C., Kay, C., Thomas, R., Porter, J., Stapleton, C. M.,
597 and Moore, H. (2010). “Evaluating short-term changes in recreational water quality during
598 a hydrograph event using a combination of microbial tracers, environmental microbiology,

599 microbial source tracking and hydrological techniques: A case study in southwest wales, uk.”
600 *Water Res.*, 44(16), 4783–4795.

601 Zhang, J., Qiu, H., Li, X., Niu, J., Nevers, M. B., Hu, X., and Phanikumar, M. S. (2018). “Real-time
602 nowcasting of microbiological water quality at recreational beaches: a wavelet and artificial
603 neural network based hybrid modelling approach.” *Environ. Sci. Technol.*, 52, 8446–8455.

604 Zhang, Z., Deng, Z., and Rusch, K. A. (2012). “Development of predictive models for determining
605 enterococci levels at gulf coast beaches.” *Water Res.*, 46(2), 465–474.

606 **List of Tables**

607 1 Measured FIO concentrations during 22 June-28 September, 2011. Ln denotes
608 natural logarithm. 27

609 2 Measured environmental variables during 22 June-28 September, 2011. Ln denotes
610 natural logarithm. 28

611 3 Predictive variables selected by the Gamma-GA tests and stepwise MLRs 29

612 4 MSE and unadjusted R^2 between computed and measured *Enterococci* concentra-
613 tions. The best results for each Realization are bolded. 30

614 5 MSE and unadjusted R^2 between computed and measured *E Coli* concentrations.
615 The best results for each Realization are bolded. 31

TABLE 1. Measured FIO concentrations during 22 June-28 September, 2011. Ln denotes natural logarithm.

| | Variables | Ln transformation | Range after transformation | |
|-----------|---------------------------------|-------------------|----------------------------|------|
| | | | min | max |
| FIO Data: | <i>E Coli</i> (cfu/100 mL) | Yes | 1.10 | 8.04 |
| | <i>Enterococci</i> (cfu/100 mL) | Yes | 1.10 | 8.37 |

TABLE 2. Measured environmental variables during 22 June-28 September, 2011. Ln denotes natural logarithm.

| | Variables | Ln transformation | Range after transformation | |
|----------------------|--|-------------------|----------------------------|-------|
| | | | min | max |
| Stream flow data: | Washinghouse Brook (m ³ /s) | Yes | -4.71 | -0.03 |
| | Brockhole Stream (m ³ /s) | Yes | -5.30 | -1.94 |
| | Clyne River (m ³ /s) | Yes | -2.42 | 1.98 |
| | Brynmill Stream (m ³ /s) | Yes | -4.20 | 1.33 |
| | River Tawe (m ³ /s) | Yes | 0.843 | 5.15 |
| | River Neath (m ³ /s) | Yes | 0.642 | 5.03 |
| | River Afan (m ³ /s) | Yes | 0.298 | 4.23 |
| Tidal data: | Normalized Tide level at Mumbles (-) | No | -0.499 | 0.483 |
| Meteorological data: | Global radiation (W/m ²) | Yes | -1.97 | 6.86 |
| | Temperature (°C) | No | 8.92 | 23.2 |
| | Relative humidity (%) | No | 34.3 | 99.0 |
| | Rainfall (mm) | Yes | -13.8 | 0.588 |
| | Wind speed to the North (m/s) | No | -11.6 | 4.14 |
| | Wind speed to the East (m/s) | No | -5.90 | 6.64 |
| Water quality data: | Turbidity (NTU) | Yes | 0.843 | 4.97 |
| | Salinity (ppt) | No | 1.90 | 153 |

TABLE 3. Predictive variables selected by the Gamma-GA tests and stepwise MLRs

| Variables identified from the correlation analysis | <i>Enterococci</i> | | <i>E Coli</i> | |
|--|--------------------|-----------------------|---------------|-----------------------|
| | Gamma-GA test | Stepwise Linear model | Gamma-GA test | Stepwise Linear model |
| Streamflow [lag 10 h] | 1 | 0 | 0 | 1 |
| Mumbles Level [lag 2 h] | 0 | 0 | 0 | 0 |
| Mumbles Level [lag 4 h] | 1 | 0 | 1 | 1 |
| Mumbles Level [lag 6 h] | 1 | 1 | 1 | 0 |
| Global Radiation [lag 2 h] | 0 | 1 | 0 | 1 |
| Global Radiation [lag 4 h] | 0 | 0 | 1 | 0 |
| Global Radiation [lag 6 h] | 1 | 0 | 0 | 0 |
| Temperature [lag 2 h] | 1 | 0 | 0 | 1 |
| Temperature [lag 6 h] | 1 | 0 | 1 | 0 |
| Relative Humidity [lag 2 h] | 0 | 1 | 0 | 1 |
| Relative Humidity [lag 8 h] | 1 | 0 | 1 | 0 |
| Cum. of Rain [lag 2 h] | 0 | 0 | 0 | 0 |
| Cum. of Rain [lag 3 h] | 0 | 0 | 0 | 0 |
| Cum. of Rain [lag 4 h] | 0 | 0 | 0 | 0 |
| Cum. of Rain [lag 6 h] | 0 | 0 | 0 | 0 |
| Cum. of Rain [lag 8 h] | 0 | 0 | 0 | 0 |
| Cum. of Rain [lag 10 h] | 0 | 0 | 0 | 0 |
| Cum. of Rain [lag 12 h] | 0 | 1 | 0 | 0 |
| Wind Speed N [lag 2 h] | 0 | 1 | 1 | 1 |
| Wind Speed N [lag 6 h] | 0 | 0 | 1 | 0 |
| Wind Speed N [lag 10 h] | 0 | 1 | 0 | 1 |
| Wind Speed E [lag 2 h] | 1 | 1 | 1 | 1 |
| Wind Speed E [lag 10 h] | 0 | 1 | 0 | 0 |

"1" denotes selected and "0" denotes not-selected.

TABLE 4. MSE and unadjusted R^2 between computed and measured *Enterococci* concentrations. The best results for each Realization are bolded.

| Realization 1 | | | | | | | |
|---------------|-----------------------|---------------|---------------|---------------|---------------|---------------|---------------|
| | Hidden layer node no. | MSE | | | R^2 | | |
| | | Training | Validation | Testing | Training | Validation | Testing |
| GG-ANN | 35 | 0.0074 | 0.0157 | 0.0214 | 0.8369 | 0.6654 | 0.5361 |
| SL-ANN | 11 | 0.0210 | 0.0232 | 0.0260 | 0.5400 | 0.5079 | 0.4357 |
| GG-Linear | N/A | | 0.0357 | 0.0399 | | 0.2224 | 0.1348 |
| SL-Linear | N/A | | 0.0311 | 0.0328 | | 0.3235 | 0.2883 |
| Realization 2 | | | | | | | |
| | Hidden layer node no. | MSE | | | R^2 | | |
| | | Training | Validation | Testing | Training | Validation | Testing |
| GG-ANN | 38 | 0.0134 | 0.0172 | 0.0227 | 0.7177 | 0.6025 | 0.4993 |
| SL-ANN | 6 | 0.0257 | 0.0194 | 0.0295 | 0.4542 | 0.5518 | 0.3611 |
| GG-Linear | N/A | | 0.0368 | 0.0352 | | 0.2021 | 0.2246 |
| SL-Linear | N/A | | 0.0312 | 0.0322 | | 0.3229 | 0.2895 |
| Realization 3 | | | | | | | |
| | Hidden layer node no. | MSE | | | R^2 | | |
| | | Training | Validation | Testing | Training | Validation | Testing |
| GG-ANN | 40 | 0.0071 | 0.0188 | 0.0199 | 0.8292 | 0.6457 | 0.6156 |
| SL-ANN | 12 | 0.0192 | 0.0243 | 0.0225 | 0.5385 | 0.5418 | 0.5699 |
| GG-Linear | N/A | | 0.0359 | 0.0393 | | 0.1944 | 0.2403 |
| SL-Linear | N/A | | 0.0320 | 0.0293 | | 0.2812 | 0.4337 |

TABLE 5. MSE and unadjusted R^2 between computed and measured *E Coli* concentrations. The best results for each Realization are bolded.

| Realization 1 | | | | | | | |
|---------------|--------------------------|---------------|---------------|---------------|---------------|---------------|---------------|
| | Hidden layer node no. | MSE | | | R^2 | | |
| | | Training | Validation | Testing | Training | Validation | Testing |
| GG-ANN | 25 | 0.0067 | 0.0159 | 0.0214 | 0.8396 | 0.6077 | 0.5312 |
| SL-ANN | 18 | 0.0096 | 0.0154 | 0.0174 | 0.7705 | 0.6198 | 0.6177 |
| GG-Linear | N/A | | 0.0325 | 0.0342 | | 0.2166 | 0.2482 |
| SL-Linear | N/A | | 0.0297 | 0.0305 | | 0.2838 | 0.3290 |
| Realization 2 | | | | | | | |
| | Hidden layer node no. | MSE | | | R^2 | | |
| | | Training | Validation | Testing | Training | Validation | Testing |
| GG-ANN | 13 | 0.0119 | 0.0178 | 0.0205 | 0.7208 | 0.5939 | 0.4801 |
| SL-ANN | 18 | 0.0113 | 0.0135 | 0.0188 | 0.7370 | 0.6914 | 0.5221 |
| GG-Linear | N/A | | 0.0331 | 0.0315 | | 0.2294 | 0.1996 |
| SL-Linear | N/A | | 0.0299 | 0.0295 | | 0.3041 | 0.2484 |
| Realization 3 | | | | | | | |
| | Hidden layer node no. | MSE | | | R^2 | | |
| | | Training | Validation | Testing | Training | Validation | Testing |
| GG-ANN | 25 | 0.0073 | 0.0146 | 0.0196 | 0.8066 | 0.6747 | 0.6337 |
| SL-ANN | 27 | 0.0091 | 0.0155 | 0.0186 | 0.7582 | 0.6539 | 0.6501 |
| GG-Linear | N/A | | 0.0321 | 0.0363 | | 0.1873 | 0.3181 |
| SL-Linear | N/A | | 0.0297 | 0.0310 | | 0.2501 | 0.4167 |

616
617
618
619
620
621
622
623
624
625
626
627
628
629
630
631
632
633
634
635
636
637

List of Figures

| | | |
|---|--|----|
| 1 | Flow chart for the modelling approach. | 33 |
| 2 | (2a) Site layout and key sampling locations in Swansea Bay, UK. (2b) A close-up of Designated Sampling Points (DSPs, in purple) in the sampling transect in Figure 2a in the 2011 bathing season at 30-minute intervals from 07:00 to 16:00. Base map: (2a) Esri; (2b) Google Earth. | 34 |
| 3 | M-test results for (3a) <i>Enterococci</i> , Realization 3 and (3b) <i>E Coli</i> , Realization 1. . . | 35 |
| 4 | Mean squared errors (MSEs) for the (4a) training, (4b) validation, and (4c) testing sets of GG-ANN and SL-ANN models versus number of hidden layer nodes for <i>Enterococci</i> , Realization 3. | 36 |
| 5 | Mean squared errors (MSEs) for the (5a) training, (5b) validation, and (5c) testing sets of GG-ANN and SL-ANN models versus number of hidden layer nodes for <i>E Coli</i> , Realization 1. | 37 |
| 6 | Regressions between target <i>Enterococci</i> concentrations and GG-ANN model outputs for (6a) training; (6b) validation; (6c) testing; and (6d) all data sets, Realization 3. LCC: Linear correlation coefficient. | 38 |
| 7 | Regressions between target <i>E Coli</i> concentrations and GG-ANN model outputs for (7a) training; (7b) validation; (7c) testing and (7d) all data sets, Realization 1. LCC: Linear correlation coefficient. | 39 |
| 8 | Performance tables for data-driven models; (left) <i>Enterococci</i> , Realization 1, testing sets; (right) <i>E Coli</i> , Realization 3, testing sets. (8a, 8b) GG-ANN models; (8c, 8d) SL-ANN models; (8e, 8f) GG-Linear models; (8g, 8h) SL-Linear models. | 40 |

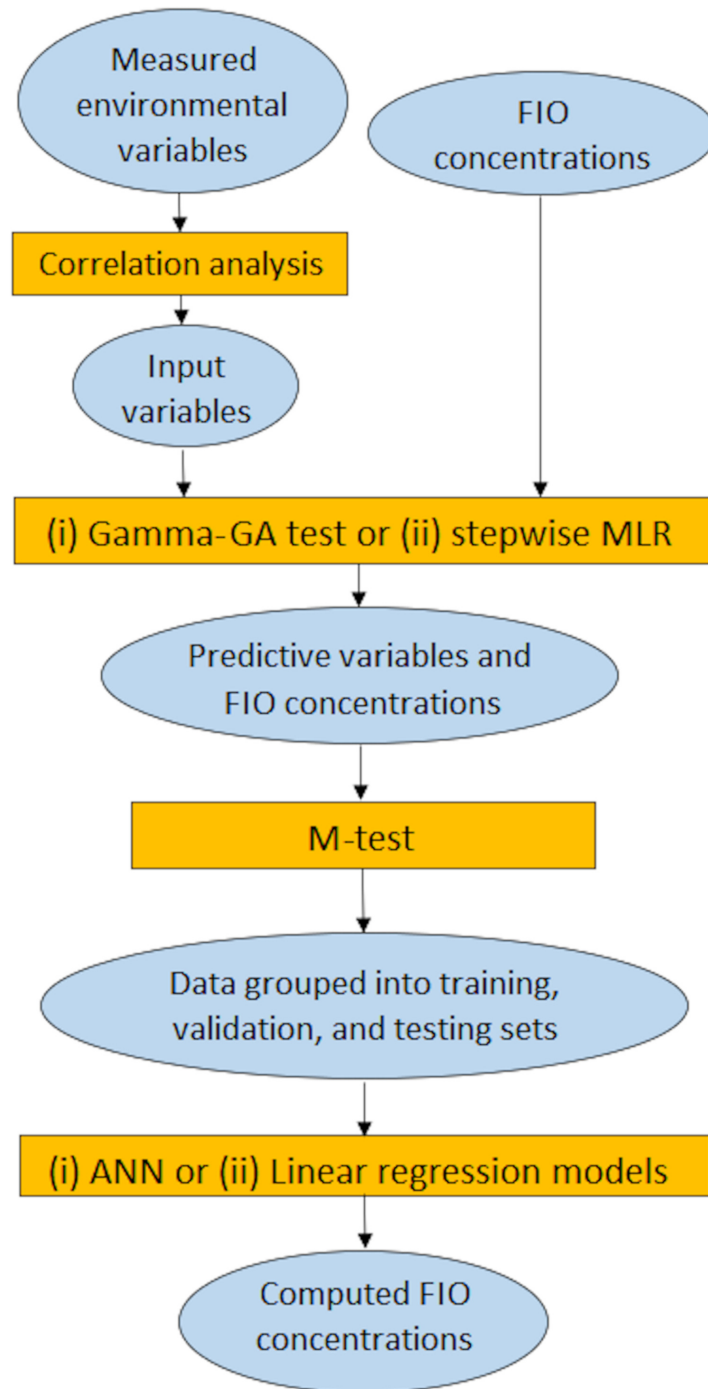
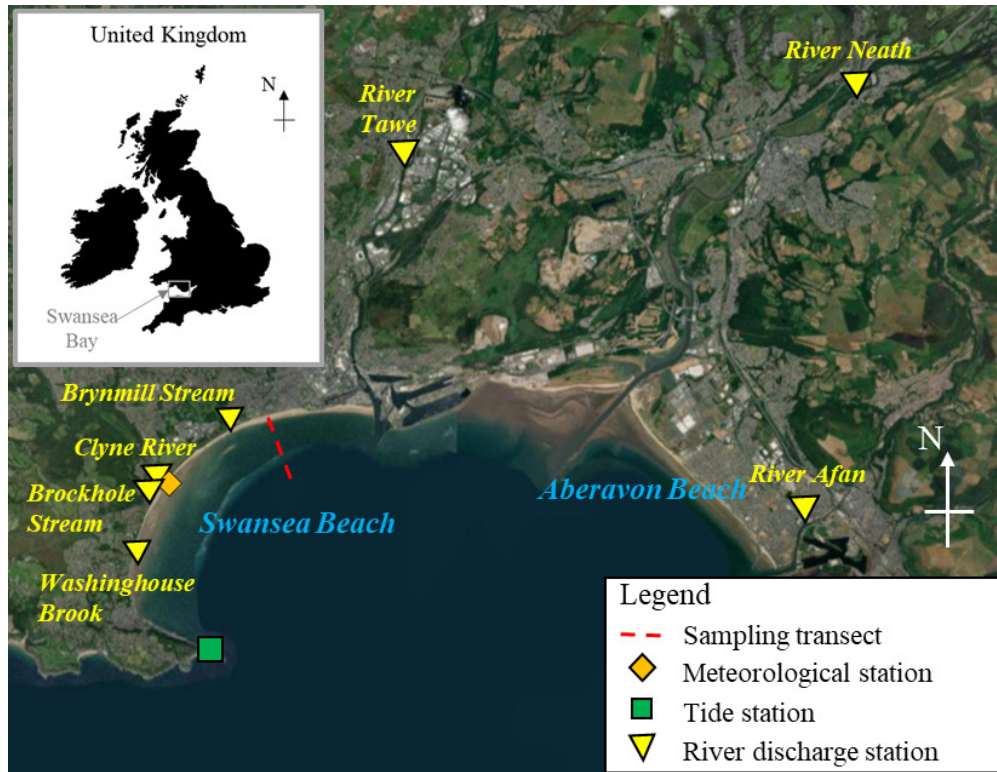
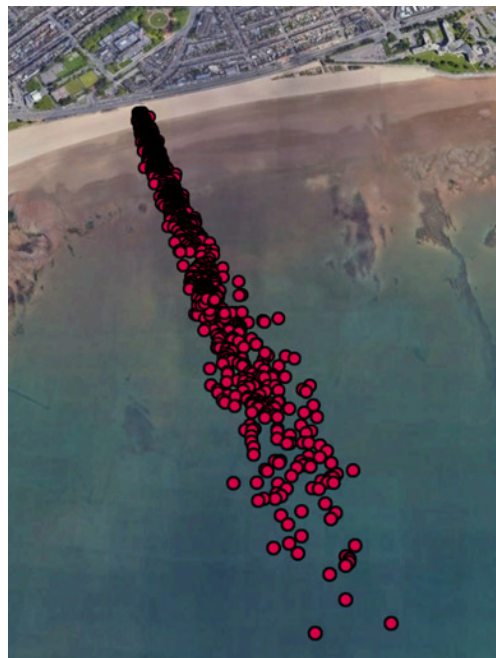


Fig. 1. Flow chart for the modelling approach.

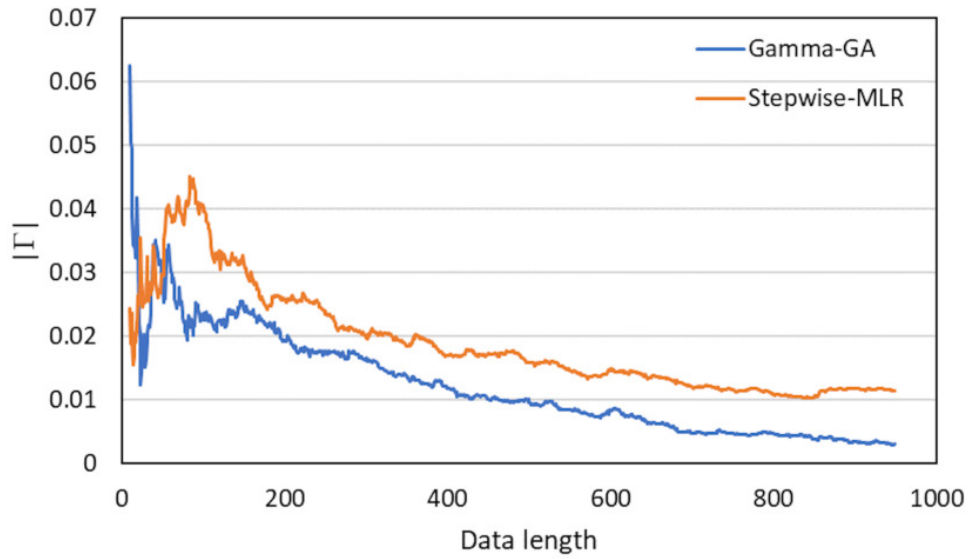


(a)

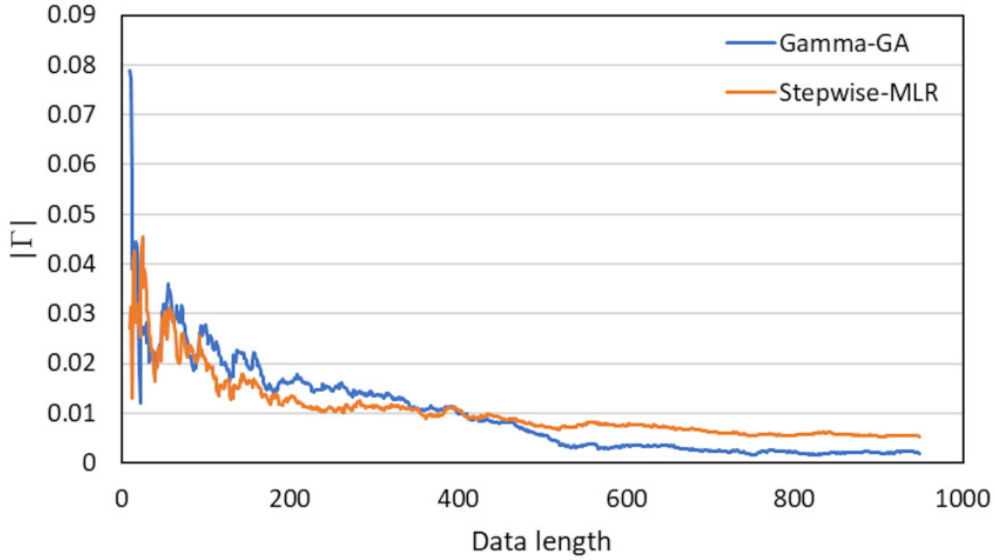


(b)

Fig. 2. (2a) Site layout and key sampling locations in Swansea Bay, UK. (2b) A close-up of Designated Sampling Points (DSPs, in purple) in the sampling transect in Figure 2a in the 2011 bathing season at 30-minute intervals from 07:00 to 16:00. Base map: (2a) Esri; (2b) Google Earth.

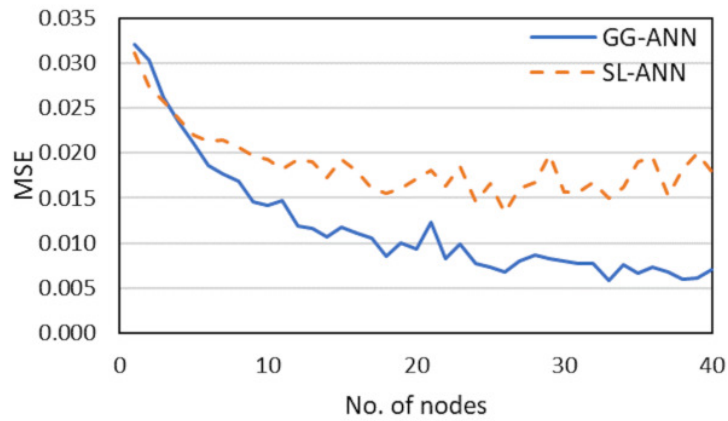


(a)

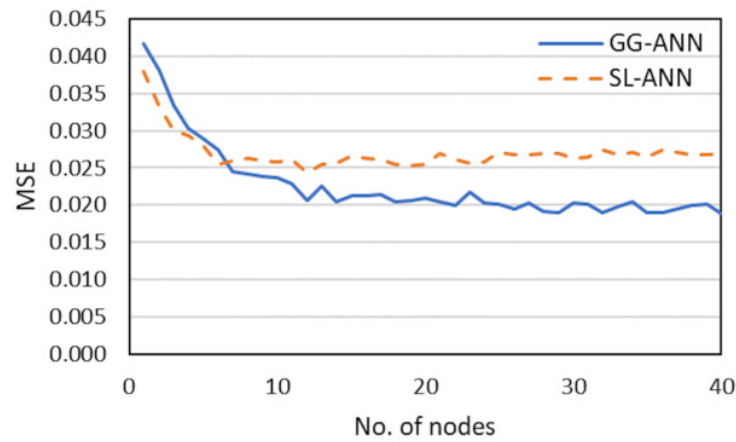


(b)

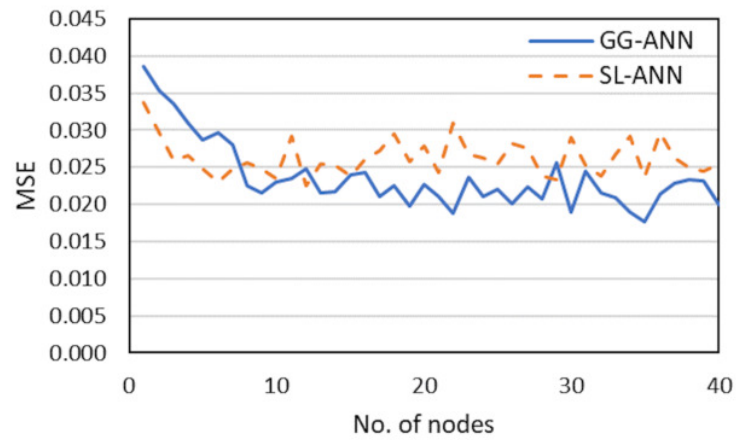
Fig. 3. M-test results for (3a) *Enterococci*, Realization 3 and (3b) *E Coli*, Realization 1.



(a)

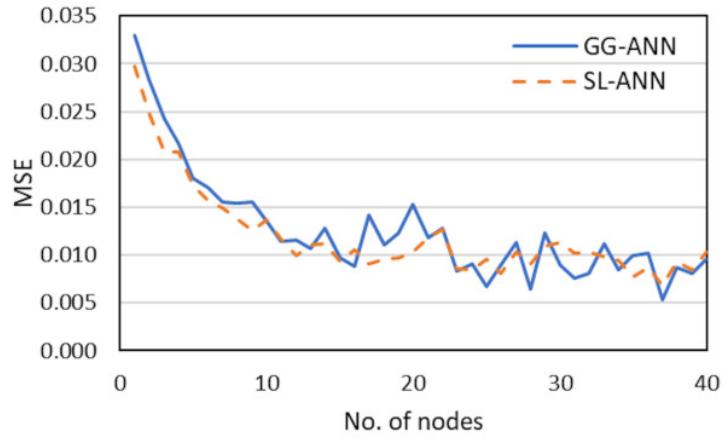


(b)

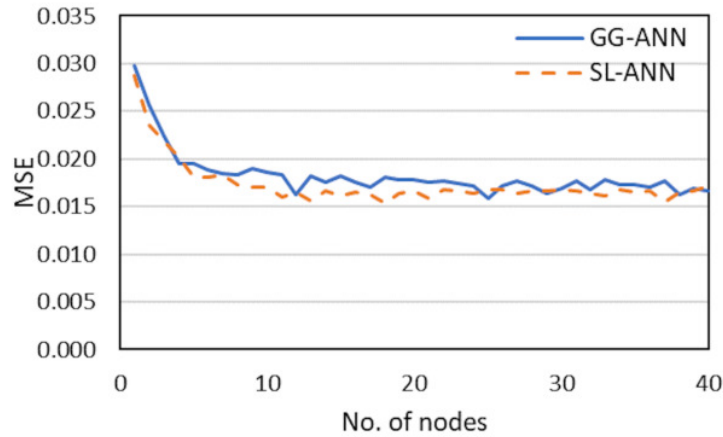


(c)

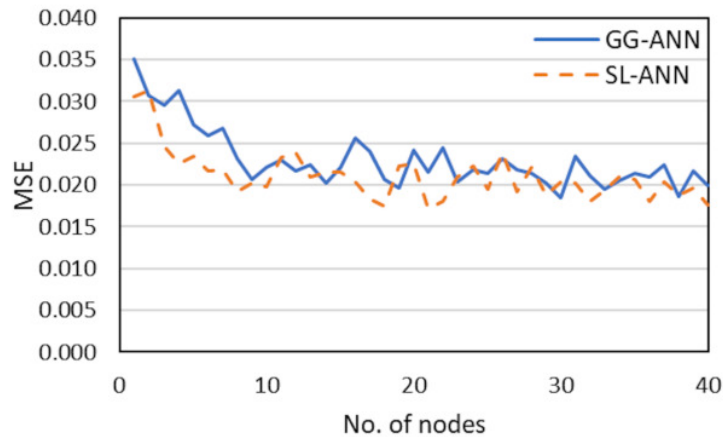
Fig. 4. Mean squared errors (MSEs) for the (4a) training, (4b) validation, and (4c) testing sets of GG-ANN and SL-ANN models versus number of hidden layer nodes for *Enterococci*, Realization 3.



(a)



(b)



(c)

Fig. 5. Mean squared errors (MSEs) for the (5a) training, (5b) validation, and (5c) testing sets of GG-ANN and SL-ANN models versus number of hidden layer nodes for *E Coli*, Realization 1.

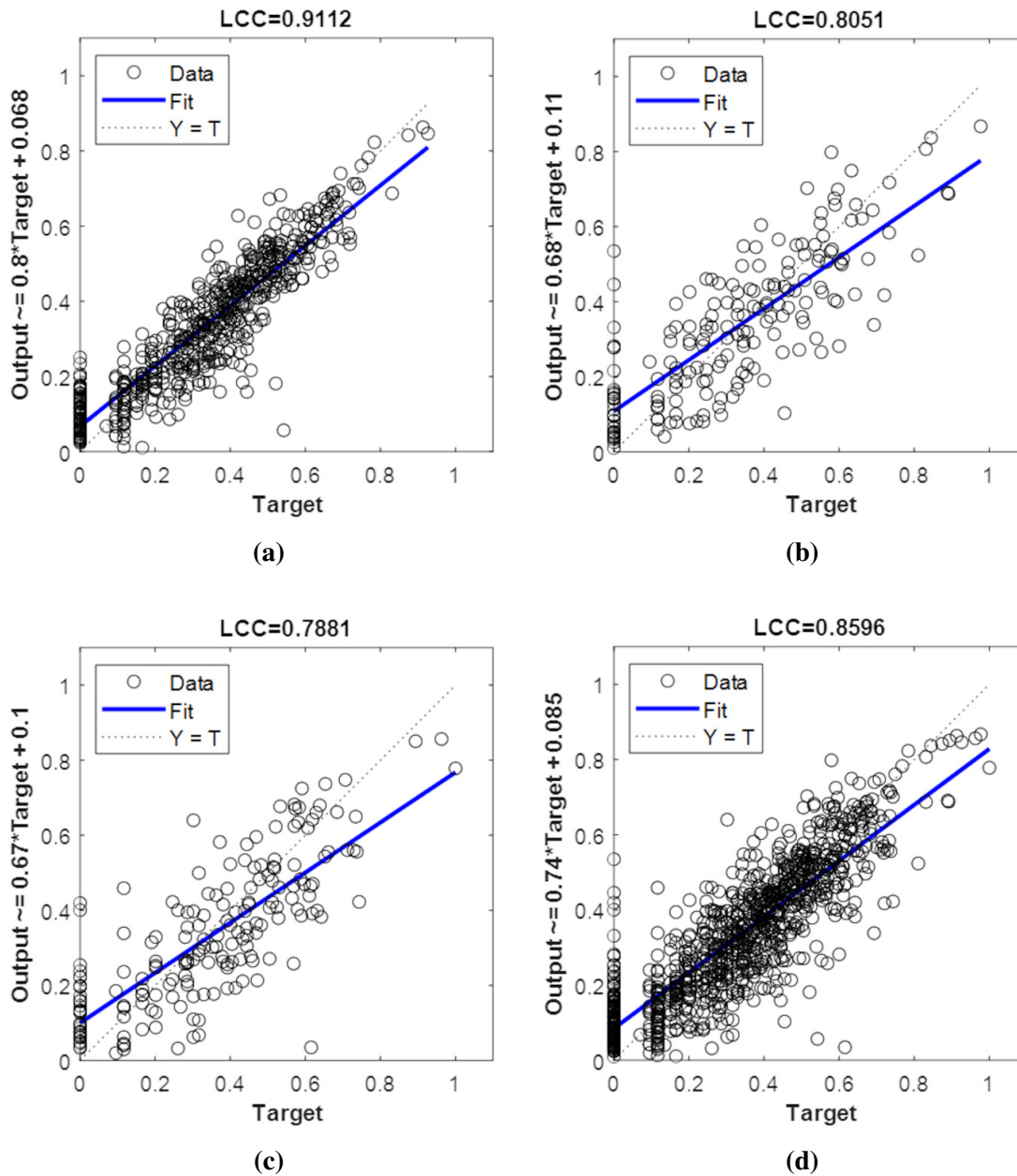


Fig. 6. Regressions between target *Enterococci* concentrations and GG-ANN model outputs for (6a) training; (6b) validation; (6c) testing; and (6d) all data sets, Realization 3. LCC: Linear correlation coefficient.

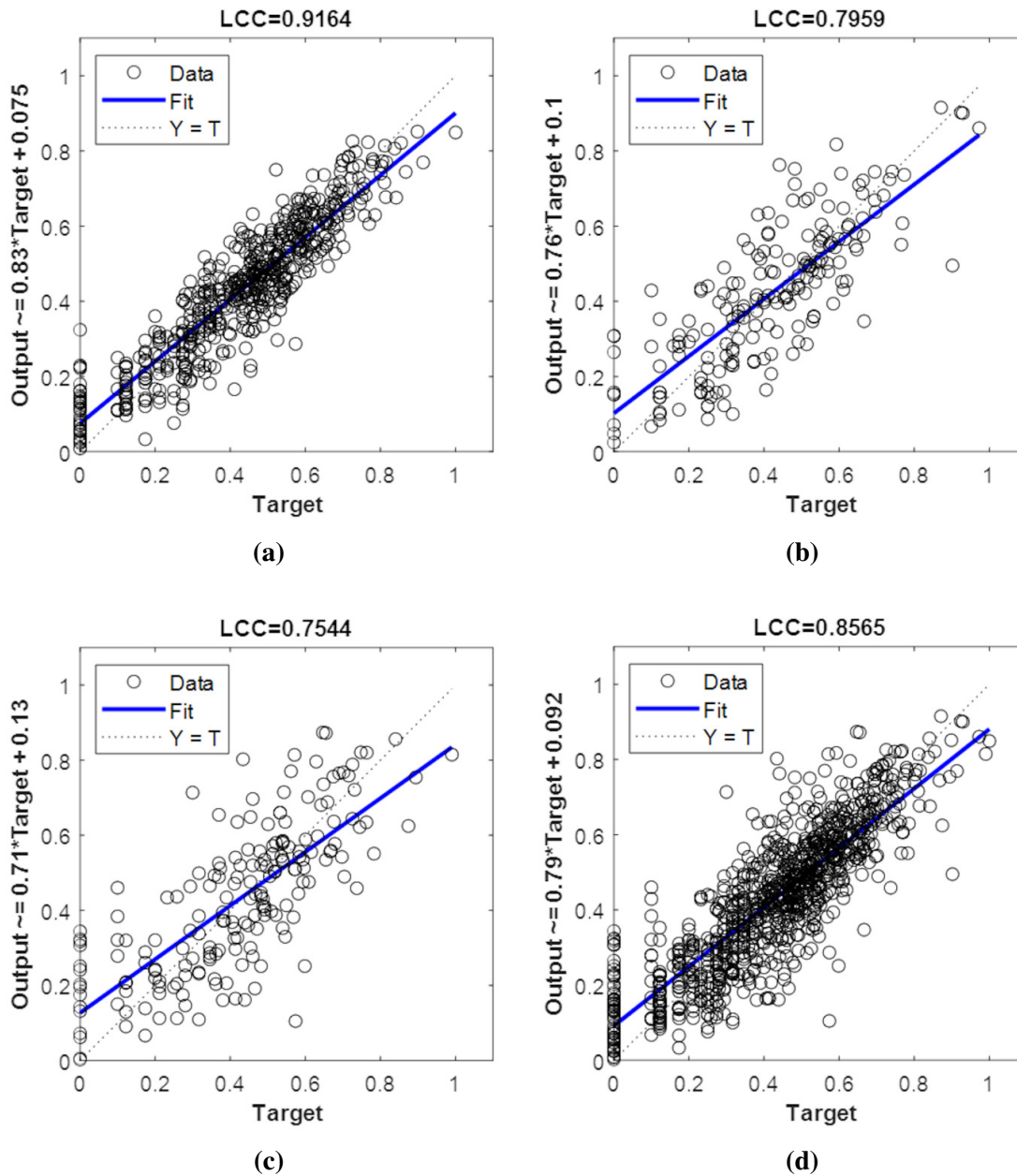


Fig. 7. Regressions between target *E Coli* concentrations and GG-ANN model outputs for (7a) training; (7b) validation; (7c) testing and (7d) all data sets, Realization 1. LCC: Linear correlation coefficient.

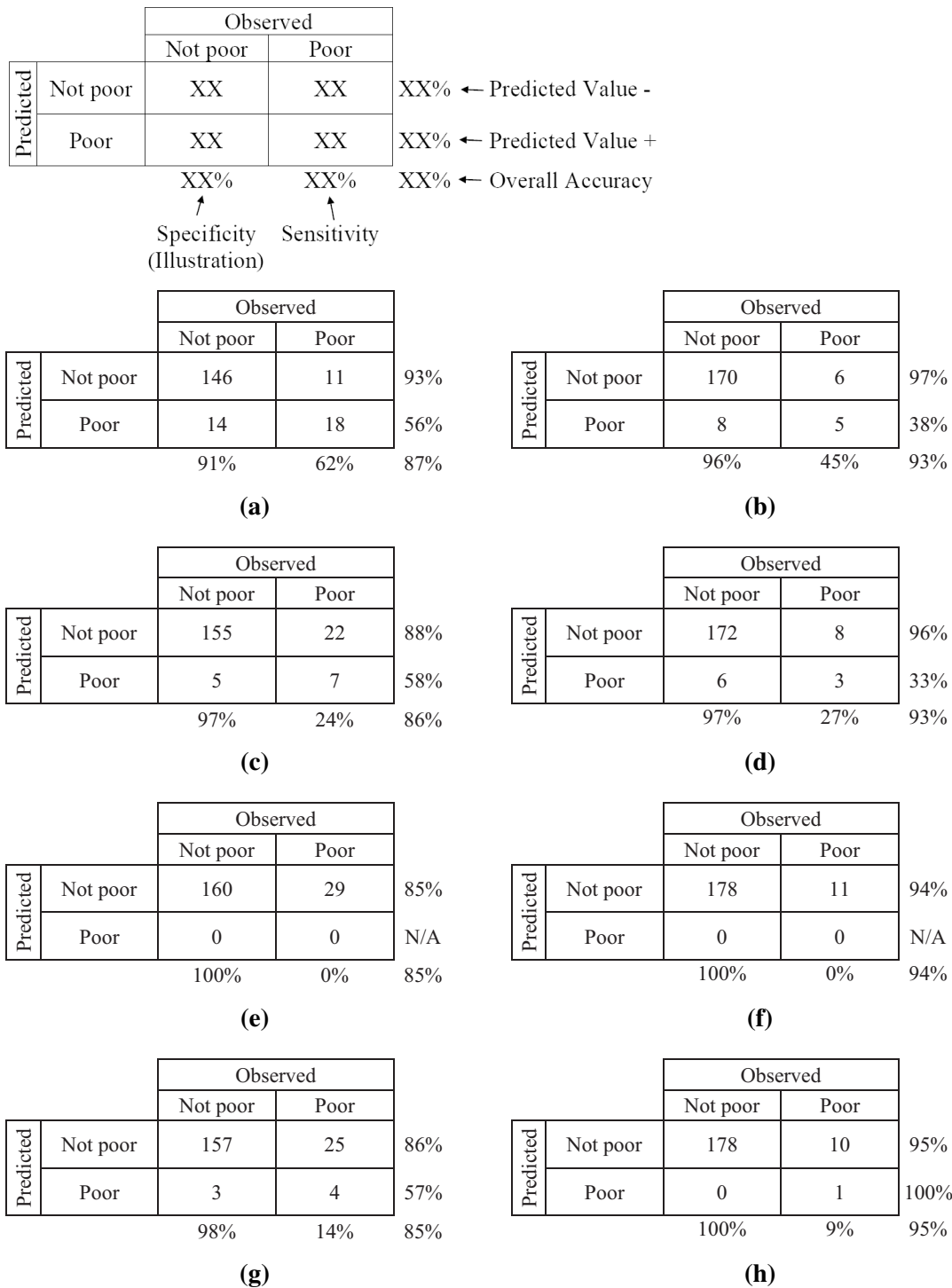


Fig. 8. Performance tables for data-driven models; (left) *Enterococci*, Realization 1, testing sets; (right) *E Coli*, Realization 3, testing sets. (8a, 8b) GG-ANN models; (8c, 8d) SL-ANN models; (8e, 8f) GG-Linear models; (8g, 8h) SL-Linear models.